Melting and alloying of Ni/Al nanolaminates induced by shock loading: A molecular dynamics simulation study

Shijin Zhao,[1] Timothy C. Germann,[2] and Alejandro Strachan[3]
[1]*Theoretical Division, Los Alamos National Laboratory, Los Alamos, New Mexico 87545, USA*
[2]*Applied Physics Division, Los Alamos National Laboratory, Los Alamos, New Mexico 87545, USA*
[3]*School of Materials Engineering, Purdue University, West Lafayette, Indiana 47907, USA*
(Received 18 July 2007; published 14 September 2007)

We demonstrate that shock-induced melting can play a key role in accelerating the initiation and propagation of self-sustained exothermic alloying reactions in nanostructured Ni/Al nanolaminates. Following a pronounced increase of the local pressure upon melting, due to structural expansion, enhanced material diffusion and intermixing around the molten regions accelerate self-sustained alloying reactions, leading to a pressure decrease. This competition between melting and alloying reactions leads to an oscillatory overall pressure as the melting and alloy formation fronts propagate.

DOI: 10.1103/PhysRevB.76.104105 PACS number(s): 62.50.+p, 47.40.Nm, 82.40.Fp

I. INTRODUCTION

Despite tremendous research efforts to understand shock-induced chemical, mechanical, and thermal processes in energetic materials for tens of years, the interplay between these processes, such as shock-induced melting and exothermic reactions, remains to be characterized. This situation stems from the very fast and complex processes involved, which usually occur in a very short time (picoseconds) at elevated temperatures and very high pressures. Multilayer reactive foils are an attractive prototype for investigating the interactions between these processes, with their simplified geometry providing well-defined interfaces at which various shock-induced processes such as melting, alloying, and chemical reactions can be monitored. In addition, their nonporous structure allows only a competition between mass and thermal diffusion. The self-propagating exothermic alloying reactions observed in Ni/Al, Ti/Al, and other such nanosized multilayer foils have velocities up to 30 m/s, leading to temperatures of 1500 K or more.[1] Such nanolaminates have recently been developed commercially as local heat sources to solder or otherwise join components.[2,3] In contrast to the standard spark or thermal initiation of a reaction front along the foil used in these applications, here we will consider the possibility of shock initiation normal to the multilayer planes. In this situation, the initial rapid shock compression and heating are followed by melting and alloying reactions, which are propagated by thermal and mass diffusion.

Nonequilibrium molecular dynamics (MD) simulations of shock loading of materials provide an accurate description of the loading process but, in most cases, have been limited to relatively short times dictated by the shock velocity and length of the target sample.[4–6] Equilibrium methods have been derived to characterize longer-time phenomena caused by shock loading;[7–10] these methods correctly describe the state of the system after the passage of the shock, but the nonequilibrium loading phenomena are described in an artificial manner. Here, we use a recently developed method that couples accurate descriptions of both the initial nonequilibrium shock loading process and also any subsequent long-time phenomena.[11]

II. SIMULATION MODEL AND METHOD

Figure 1 shows the initial configuration consisting of a Ni/Al multilayer composite (both the [111] direction boundary and the central impact plane are located at the midpoint of an Al layer). The unequal Ni and Al layer thicknesses are set up such that the final stoichiometry is very close to Ni_3Al (each bilayer contains 47 628 Ni atoms and 15 552 Al); the interfaces are perfectly planar (111) surfaces and the composite will be shocked along the [111] direction. The interatomic interactions are described by an embedded atom method (EAM) potential developed by Mishin *et al.*,[12] which was constructed using experimental data and a large set of *ab initio* linearized augmented plane wave structural energies. This potential provides an accurate description of thermal expansion, diffusion, and equations of state for Al, Ni, and their alloys, which is of great importance for nonequilibrium atomistic simulations.

The Ni/Al composite, initially containing a 1 nm gap, collides with a relative velocity of $2u_p$ (see Fig. 1; the particle, or piston, velocity u_p is 2 nm/ps in this paper). Periodic boundary conditions are imposed in all three dimensions, with a shrinking boundary condition (the left boundary

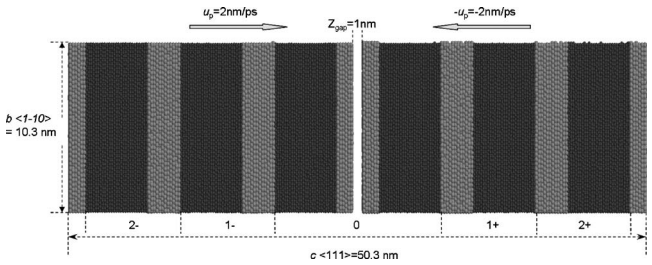

FIG. 1. Schematic of the simulation geometry. The length in $a\langle 11-2\rangle$ (the direction perpendicular to the paper) is 8.9 nm. The sample includes $N_{Ni}+N_{Al}=379\,080$ atoms with $N_{Ni}\sim 3N_{Al}$. The location of each Ni/Al bilayer is indicated in the figure. "+" and "−" before the piston velocity denote the moving directions of the left part (pointing to the right hand) and the right part (to the left hand) of the sample.

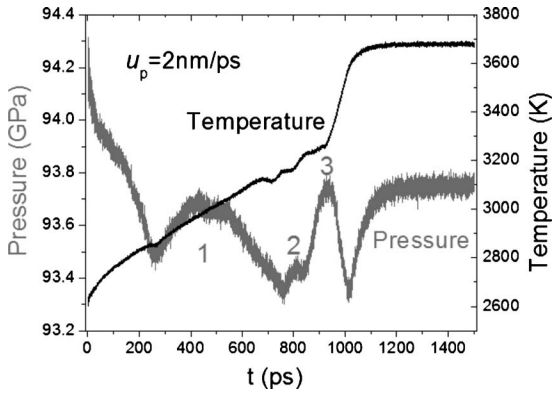

FIG. 2. Overall temperature and pressure as a function of time in *NVE* run for the Ni/Al nanolaminates after a shock loading at u_p=2 nm/ps has finished. The numbers in the overall pressure profile denote the three peaks of the pressure seen in the simulation.

moving at $+u_p$ and the right boundary at $-u_p$) imposed in the [111] shock direction to avoid a discontinuity in the velocity field as the slab collides at the midpoint. Details of the simulation technique can be found in Ref. 11. Upon collision, two shock waves (with particle velocity u_p relative to the uncompressed material) propagate outward in opposite directions, leaving behind a shocked material with zero translational velocity if the material is homogeneous.[11] Just at the critical time[11] when all the material in the simulation cell has been shocked and the outgoing shock waves meet at the [111] periodic boundary, we stop the shrinking boundary condition and begin a constant volume and energy (*NVE*) MD run to follow the longer-time-scale alloying initiation and propagation. To monitor the time evolution of local properties, we divide the sample into several bins along the longitudinal shock direction. We monitor the local temperature, stress tensor, and other properties in each bin as well as the average temperature and pressure of the entire system.

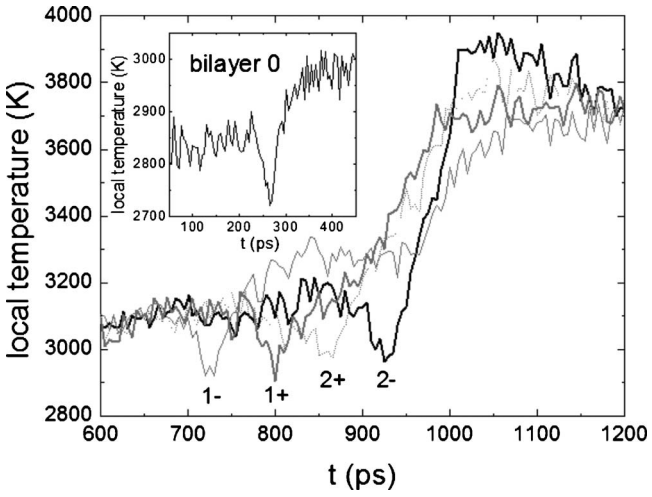

FIG. 3. Temporal evolution of the local temperature in respective Ni/Al bilayers denoted in Fig. 1. Inset shows the temporal evolution of the local temperature in bilayer 0.

III. RESULTS AND DISCUSSIONS

Figure 2 shows the temporal evolution of the overall system's temperature and pressure during the *NVE* portion of the simulation. For the first 265 ps, the overall temperature continually increases due to heating from repeated wave reflections between Ni/Al interfaces[11] and energy release from solid-state alloying reactions confined to a narrow region around the interfaces, which also lower the pressure. At 265 ps, the overall temperature plateaus for about 40 ps before continuing its increase. We examined the local temperature (inset of Fig. 3), the local structure [Fig. 4(a)], and the pair distribution function $g_{\mathrm{tot}}(r)$, which are compared to $g_{\mathrm{tot}}(r)$ of the compressed NiAl liquid having the same density in Fig. 4(b) and found that the central bilayer (i.e., bilayer 0 in Fig. 1) melts at 265 ps, removing heat from the system. As time evolves, we observe a sequential propagation of melting transitions occurring in bilayers 1− at 720 ps, 1+ at 800 ps, 2+ at 860 ps, and 2− at 925 ps; finally, at 1020 ps, the periodic Al boundaries become liquid. Such sequential melting processes of the various layers also give rise to the small kinks evident in the overall temperature (Fig. 2), as clearly shown by the sudden decrease of the local temperature (Fig. 3) of each bilayer upon melting (i.e., the latent heat of melting). It is very interesting to note that the melt-

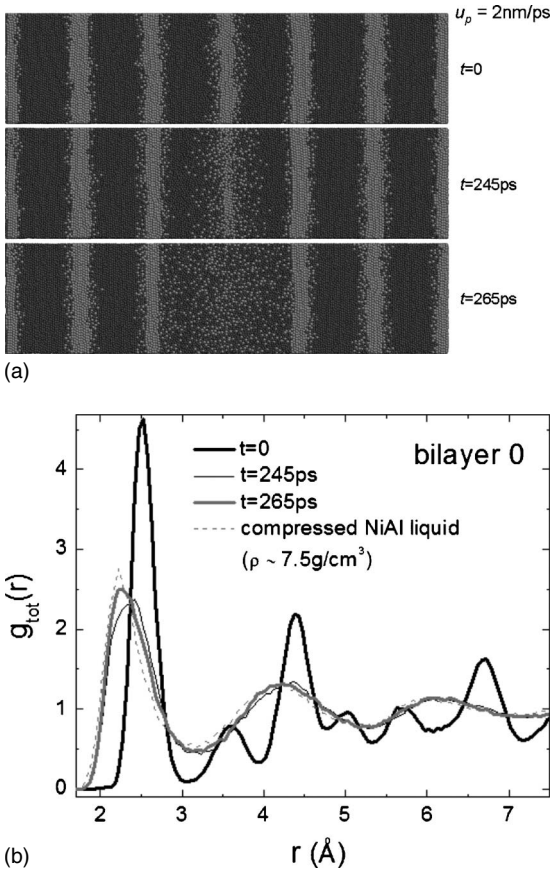

FIG. 4. Temporal evolution of (a) snapshots of the configuration and (b) total radial distribution function $g_{\mathrm{tot}}(r)$ indicating a melting process occurring in bilayer 0 under shock loading at u_p =2 nm/ps.

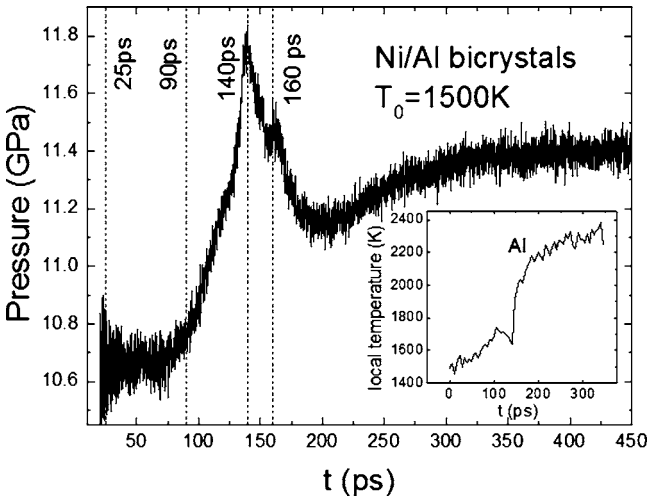

FIG. 5. Overall pressure as a function of time for the small Ni/Al bicrystal system in *NVE* run, which is assigned an initial temperature of 1500 K. Inset shows the temporal evolution of the local temperature in the Al layer.

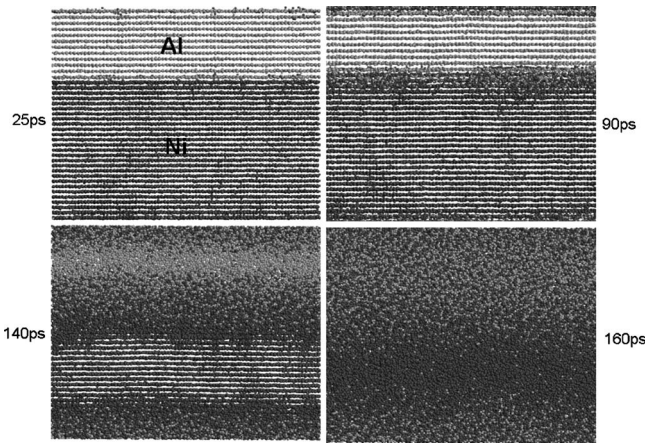

FIG. 6. Snapshots of the configuration of the small Ni/Al bicrystal system at several times, showing structural disorder and melting processes of Al and Ni layers.

ing, propagating from the center to the sides, is well confined between two symmetric Al layers: only after the melting of the entire central bilayer has finished does the melting of bilayers 1− and 1+ start [Fig. 4(a)], and so on. We examined the local pressure as a function of time and position in the shock direction and found that a higher local pressure is generated around the Al layers and Al/Ni interfaces inhibiting the melting of these compressed Al layers. However, once an Al layer melts, the exothermic alloying with the neighboring Ni layer rapidly causes that Ni layer to melt, causing the melting and alloy formation to copropagate from one Ni/Al bilayer to the next in an irregular "hiccup" fashion. This also leads to the unusual features seen in the overall pressure profile: three peaks of the pressure (denoted as "1," "2," and "3" in Fig. 2) appear around the times when the melting transitions occur.

To isolate the effects of melting and alloying on the temporal evolution of temperature and pressure, we simulate a smaller system containing only one Ni/Al bilayer. The sizes of the Ni and Al layers in the small system are the same as in the shocked Ni/Al nanolaminates (i.e., with width $c\langle 111\rangle = 8.2$ nm and containing 47 628 Ni and 15 552 Al atoms). The small Ni/Al bilayer system is assigned an initial temperature of 1500 K and allowed to evolve in the microcanonical (*NVE*) ensemble. Once again, a pronounced peak is observed in the temporal evolution of the overall pressure (Fig. 5), presumably indicating a melting transition.

To confirm this and explore the interplay between melting and alloying, we calculate the local temperature in the Al layer as a function of time. The inset of Fig. 5 shows that this local temperature slowly increases for the first 75 ps, then continues to rise with a slightly larger slope before suddenly dropping at $t \sim 140$ ps, and subsequently increases rapidly again. This indicates that the alloying reactions start from the very beginning but are greatly accelerated by a structural disorder and melting transition starting at $t=75$ ps in the Al layer. When we monitor the temporal evolution of the local structure, we find that a thermal structural disordering of the Ni/Al interface begins at $t \sim 75$ ps, and a melting of the Al layer is completed at 140 ps (see the snapshots in Fig. 6; the local temperature drops around 140 ps because the latent heat of melting is more dominant than the heat release from alloying reactions). Since the total volume of the system is constant, the structural expansion upon the disordering and melting keeps the overall pressure increasing between 75 and 140 ps. After the melting of the Al layer is completed at 140 ps, the local temperature rapidly increases due to (i) faster chemical reactions and energy release rates in the liquid due to increased atomic mobility and (ii) the energy released from the alloying reactions is only going toward increasing the temperature and no longer into melting. When the exothermic reactions become dominant at $t > 140$ ps, the pressure begins dropping off (Fig. 5) because both the potential energy of the system and its contribution to the pressure decrease in the alloying reactions.

We now return to the temporal evolution of the overall pressure (i.e., Fig. 2) in the shocked Ni/Al nanolaminates containing six Ni/Al bilayers. As we described above, the central bilayer becomes liquid at 265 ps. When $t > 265$ ps, the disordering and melting penetrate the symmetric Al layers in bilayers 1− and 1+ and starts to propagate from the center to the sides; the pressure rises due to a structural expansion upon disordering and melting. On the other hand, the exothermic alloying reactions in the central bilayer, which start from the very beginning, tend to decrease the pressure. So, there is a competition between pressure variations from expansion upon disordering and melting and from exothermic reactions, and whether the overall pressure rises or falls is determined by such a competition. Let us focus on the dynamics in the central bilayer, between 265 and 760 ps in Fig. 2 (labeled 1 in the pressure profile). The increase of pressure due to expansion upon disordering and melting is dominant between 265 and 400 ps but is balanced by the decrease of pressure from exothermic alloying reactions from 400 to 550 ps, leading to a plateau in the overall pressure. The exothermic alloying reactions are further accelerated due to increased atomic mobility around the molten re-

gions, causing a pressure drop between 550 and 760 ps.

At later times, following sequential shock-induced melting in bilayers 1−, 1+, 2+, and 2−, the structural expansion becomes more significant and the overall pressure tends to increase. On the other hand, melting greatly accelerates the local exothermic alloying reactions, which tends to decrease the pressure. So, there is a keen competition between them during this time, leading to two additional peaks between 760 and 925 ps in the pressure profile (denoted as 2 and 3 in Fig. 2). The overall pressure goes down when the exothermic alloying reactions become dominant and vice versa. Before 925 ps, because the exothermic alloying reactions are still confined in some Ni/Al bilayers, the overall temperature increases slowly, although the local temperature in the respective Ni/Al bilayer rapidly increases. After bilayer 2− melts at 925 ps, however, the exothermic alloying reactions cannot be confined anymore because the last Ni/Al bilayer in this periodic system is surrounded by hot, already reacted materials (i.e., see Fig. 3: the local temperature of bilayer 2− has increased about 1000 K between 925 and 1005 ps). This leads to the overall explosive alloying reactions in the system, and the overall temperature increases rapidly and the pressure decreases steeply. As we see from Fig. 2, the overall explosive alloying reaction is a very fast process, which is accomplished in around 100 ps. We examine the atomic structure [Fig. 7(a)] of the whole sample at $t=1.5$ ns, compare its pair distribution function $g_{\mathrm{tot}}(r)$ [Fig. 7(b)] with a compressed Ni_3Al liquid having the same density, and find the final reaction product is very similar to the compressed Ni_3Al liquid. In addition, we calculate the number of Ni and Al atoms for all local bins divided along the longitudinal shock direction and find that the local stoichiometry of all bins fluctuates little (±2.7%) around the stoichiometry of Ni_3Al.

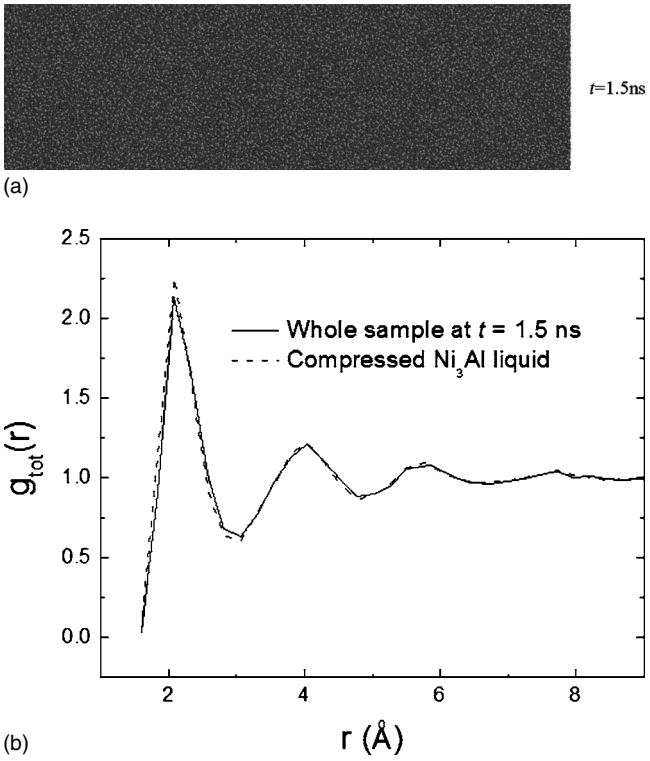

FIG. 7. (a) Snapshot of the configuration of the Ni/Al nanolaminates at $t=1.5$ ns. (b) Comparison of $g_{\mathrm{tot}}(\mathrm{r})$ of the whole sample at $t=1.5$ ns with a compressed Ni_3Al liquid having the same density.

IV. SUMMARY AND CONCLUSIONS

In summary, we observe sequential shock-induced melting processes occurring in Ni/Al multilayers by means of a recently introduced molecular dynamics technique,[11] which captures the initial shock transit as well as the subsequent long-time-scale alloying process. We find a strong interplay between the melting and alloying: The heat released from the exothermic alloying reactions facilitates the local melting, and the enhanced mobility of the molten regions accelerates the exothermic alloying reactions. On the other hand, we uncover a keen competition between the melting and alloying from the overall pressure variation: The structural expansion upon melting leads to an increase of the pressure while the alloying reactions tend to decrease the pressure.

ACKNOWLEDGMENTS

We thank Yuri Mishin for providing his EAM potential tables (Ref. 12). This work is supported by the Laboratory Directed Research and Development program (Project No. LDRD-20050343ER) at Los Alamos National Laboratory, which is operated by Los Alamos National Security, LLC (LANS) under Contract No. DE-AC52-06NA25396 with the U.S. Department of Energy.

[1] D. S. Moore, S. F. Son, and B. W. Asay, Propellants, Explos., Pyrotech. **29**, 106 (2004).
[2] B. S. Bockmon, M. L. Pantoya, S. F. Son, B. W. Asay, and J. T. Mang, J. Appl. Phys. **98**, 064903 (2005).
[3] A. B. Mann, A. J. Gavens, M. E. Reiss, D. Van Heerden, G. Bao, and T. P. Weihs, J. Appl. Phys. **82**, 1178 (1997).
[4] V. Y. Klimenko and A. N. Dremin, Sov. Phys. Dokl. **25**, 288 (1980); Prog. Astronaut. Aeronaut. **75**, 253 (1981).
[5] B. L. Holian, Phys. Rev. A **37**, 2562 (1988); B. L. Holian and P. S. Lomdahl, Science **280**, 2085 (1998); K. Kadau, T. C. Germann, P. S. Lomdahl, and B. L. Holian, *ibid.* **296**, 1681 (2002).
[6] V. V. Zhakhovskii, S. V. Zybin, K. Nishihara, and S. I. Anisimov, Phys. Rev. Lett. **83**, 1175 (1999).
[7] J. B. Maillet, M. Mareschal, L. Soulard, R. Ravelo, P. S. Lomdahl, T. C. Germann, and B. L. Holian, Phys. Rev. E **63**, 016121 (2000).
[8] E. J. Reed, L. E. Fried, and J. D. Joannopoulos, Phys. Rev. Lett. **90**, 235503 (2003).

[9] R. Ravelo, B. L. Holian, T. C. Germann, and P. S. Lomdahl, Phys. Rev. B **70**, 014103 (2004).

[10] S. Root, R. J. Hardy, and D. R. Swanson, J. Chem. Phys. **118**, 3161 (2003).

[11] S. J. Zhao, T. C. Germann, and A. Strachan, in *Shock Compression of Condensed Matter—2005*, edited by M. D. Furnish, M. Elert, T. P. Russell, and C. T. White (American Institute of Physics, Melville, NY, 2006), pp. 593–596; J. Chem. Phys. **125**, 164707 (2006).

[12] Y. Mishin, M. J. Mehl, and D. A. Papaconstantopoulos, Phys. Rev. B **65**, 224114 (2002).